Richard B. Diver
Sandia National Laboratories,
P.O. Box 5800, MS1127,
Albuquerque, NM 87185-1127
e-mail: rbdiver@sandia.gov

James E. Miller
Sandia National Laboratories,
P.O. Box 5800, MS1349,
Albuquerque, NM 87185-1349
e-mail: jemille@sandia.gov

Mark D. Allendorf
Sandia National Laboratories,
P.O. Box 969, MS9291,
Livermore, CA 04550-9291
e-mail: mdallen@sandia.gov

Nathan P. Siegel
Sandia National Laboratories,
P.O. Box 5800, MS1127,
Albuquerque, NM 87185-1127
e-mail: npsiege@sandia.gov

Roy E. Hogan
Sandia National Laboratories,
P.O. Box 5800, MS0836,
Albuquerque, NM 87185-0836
e-mail: rehogan@sandia.gov

Solar Thermochemical Water-Splitting Ferrite-Cycle Heat Engines

Thermochemical cycles are a type of heat engine that utilize high-temperature heat to produce chemical work. Like their mechanical work producing counterparts, their efficiency depends on the operating temperature and on the irreversibility of their internal processes. With this in mind, we have invented innovative design concepts for two-step solar-driven thermochemical heat engines based on iron oxide and iron oxide mixed with other metal oxide (ferrites) working materials. The design concepts utilize two sets of moving beds of ferrite reactant materials in close proximity and moving in opposite directions to overcome a major impediment to achieving high efficiency—thermal recuperation between solids in efficient countercurrent arrangements. They also provide an inherent separation of the product hydrogen and oxygen and are an excellent match with a high-concentration solar flux. However, they also impose unique requirements on the ferrite reactants and materials of construction as well as an understanding of the chemical and cycle thermodynamics. In this paper, the counter-rotating-ring receiver/reactor/recuperator solar thermochemical heat engine concept is introduced, and its basic operating principles are described. Preliminary thermal efficiency estimates are presented and discussed. Our results and development approach are also outlined.
[DOI: 10.1115/1.2969781]

Keywords: solar, thermochemical, hydrogen, metal oxide, ferrite, redox, heat engine

Introduction

Solar and nuclear energies are the world's only viable long-term energy options, and hydrogen production from these sources is potentially an environmentally advantageous long-term alternative to fossil fuels. As a result, hydrogen research is currently receiving a great deal of interest [1]. Solar power is clean and abundant and is technically capable of supplying all of the world's energy needs, utilizing a few percent of the world's desert area. Solar thermal power concentrates direct solar radiation to produce high-temperature thermal energy, which can be used in a heat engine or other thermal applications. Parabolic dish and high-performance power tower systems are capable of supplying high-temperature thermal energy [2,3]. When mass-produced, concentrating solar power systems can be cost competitive with conventional energy sources [4].

Thermochemical processes for converting solar energy into hydrogen are potentially more straightforward, more efficient, and less costly than using electric power to electrolyze water. Thermochemical cycles are heat engines that utilize high-temperature heat to produce chemical work in the form of hydrogen [5]. Like their mechanical work-producing counterparts, their efficiency depends on the operating temperature and the irreversibility of their internal processes. Thermochemical water-splitting cycles utilize a series of chemical reactions with the overall reaction $H_2O \rightarrow H_2 + 1/2O_2$. All of the other chemicals are recycled within the process. Hundreds of unique cycles have been proposed over the past 40 years, but substantial research has been done on only a few [6]. Most of the developments have envisioned nuclear heat being used as the primary heat source. As a result, temperature limitations of approximately 1000°C have resulted in most work focused on a few cycles [7]. Solar thermochemical processes offer the potential for much higher temperatures than are being considered for nuclear-based cycles.

Recent solar thermochemical research has focused on metal oxide cycles. The metal oxide cycles are attractive in that they involve fewer and less complex chemical steps than lower temperature processes, thereby resulting in less irreversibility and potentially higher cycle efficiency. The ferrite cycles utilize cyclic thermal reduction (TR) and water hydrolysis reactions with an iron-based metal oxide spinel to split water. They are particularly attractive because they involve a minimum number of steps and reactants, have solid-gas reactions, use noncorrosive materials, lend themselves to direct solar irradiation of the working material, and can avoid the recombination reactions and irreversibility associated with quenching needed with volatile-metal oxides such as zinc or cadmium oxides.

Iron oxide has been of interest since Nakamura described the FeO/Fe_3O_4 cycle [8]. The two steps in the FeO/Fe_3O_4 (iron oxide) cycle are

$$Fe_3O_4 \rightarrow 3FeO + 1/2O_2 \quad (1)$$

$$3FeO + H_2O \rightarrow Fe_3O_4 + H_2 \quad (2)$$

Reaction (1) is the TR step. It is highly endothermic and requires temperatures of over 1600 K. Reaction (2) is the water oxidation (WO) or hydrolysis step. It is slightly exothermic and is spontaneous at an ambient temperature to about 1200 K. In recent years, research has focused on mixed-metal oxides called ferrites that have a spinel crystal structure involving Fe and a second metal A (where A=Mn, Mg, Co, Zn, and/or Ni) as a way to lower the temperatures required to reduce the oxide [9–13]. Recently, Kodama et al. [14,15] and Ishihara et al. [16] demonstrated that

Contributed by the Solar Energy Engineering Division of ASME for publication in the JOURNAL OF SOLAR ENERGY ENGINEERING. Manuscript received November 9, 2007; final manuscript received December 10, 2007; published online September 4, 2008. Review conducted by Aldo Steinfeld. Paper presented at the 2006 International Solar Energy Conference (ISEC2006), Denver, CO, July 8–13, 2006.

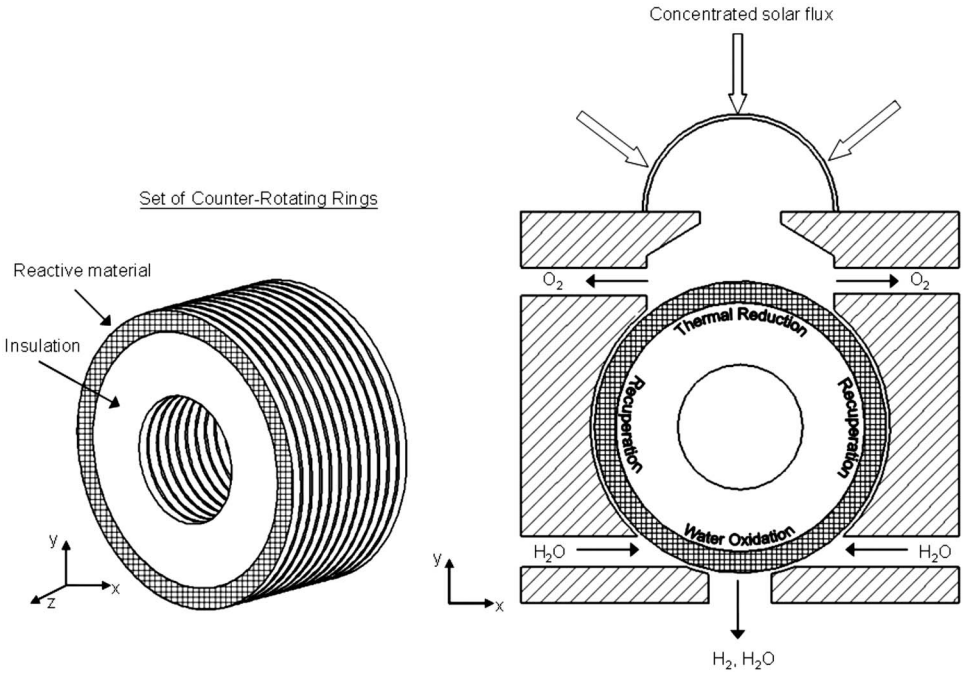

Fig. 1 Schematic of the counter-rotating-ring receiver/reactor/recuperator (CR5)

dispersing the ferrite in zirconia enhances reactivity and improves reduction and hydrolysis kinetics. They also showed that the supported materials maintain reactivity when repeatedly cycled between TR and WO reactions. Other researchers have begun to explore solar receiver/reactor designs for the ferrite cycles in which the reactant is supported on a matrix [17,18].

Recuperation of the sensible heat between the hydrolysis and reduction reactors is essential for high efficiency, especially for designs in which the ferrite is supported. Without recuperation, the energy required for sensible heating between the WO and TR temperatures is a substantial fraction of the energy input to the cycle. In addition, a significant amount of high quality sensible heat must be rejected from the cycle to cool the reactant material from the TR temperature to the WO temperature. Until recently, metal oxide thermochemical reactors have envisioned using particles. From the point of view of the receiver/reactor design, the use of particles is an obvious choice. Nakamura [8] and Steinfeld et al. [19] both recognized the need for recuperation in order to achieve high thermal performance. However, neither developed practical approaches to recuperate the heat in metal oxide particle streams. For the recently introduced matrix supported reactor designs, there is no apparent consideration of recuperation.

As in thermal-to-mechanical work producing heat engines, such as Stirling and Ericsson cycle machines, recuperation is critical. Rather than recuperate a reactor, our approach is to reactorize a recuperator. This requires developing concepts for solid-to-solid countercurrent heat exchangers and adapting them to the TR and WO reactions. This approach results in thermochemical analogs to Stirling and Ericsson cycle heat engines and provides a framework for minimizing irreversibilities. As a result, these devices are potentially efficient. However, they also place unique requirements on materials and involve numerous engineering tradeoffs. To understand and design these engines also requires an understanding of chemical and cycle thermodynamics.

The CR5 Heat Engine

To address recuperation between solids and reactor requirements for ferrite cycles, we conceived several configurations. A preferred arrangement is shown in Fig. 1. The counter-rotating-ring receiver/reactor/recuperator (CR5) uses a stack of counter-rotating rings or disks with fins along the perimeter. The fins contain a ferrite reactant, presumably on a support. Each ring rotates in the opposite direction to its neighbor at a rotational speed on the order of 1 rpm or less. The thickness of the reactant fins is a fraction of the thickness of the rings to permit solar flux to penetrate in depth and allow for water and products to be transported to and from the ferrite reactant material of the fins. Solar flux illuminates the fins on the stack of rings on the edge along nominally 1/4 of the perimeter. The moving "volumetric absorber" has the advantage of effectively smoothing nonuniform flux distributions inherent in reflective solar concentrators. In addition, because the reactant is supported, the CR5 is compatible with variable orientations relative to gravity on parabolic dishes and their relatively higher concentration ratio compared to power towers. On the opposite side of the stack, the WO reaction takes place. The remaining half of the stack (two 1/4 sections between) is adiabatic and is utilized for countercurrent recuperation, primarily by thermal radiation. Equal pressures are maintained in the two reactors to minimize flow through the recuperator sections.

As the oxidized ferrite material in the fins leaves the WO reactor and enters the recuperator, it "sees" hotter fins leaving the TR reactor on both sides. In the recuperator it heats up as the neighboring fins moving in the opposite direction cool. In the sunlit section, the concentrated solar radiation continues to heat the reactant fin and provides the heat of reaction for the endothermic TR oxygen-producing reaction as well as any additional sensible heating that is required. A vacuum pump removes the evolved oxygen. In the WO reactor, water vapor re-oxidizes the ferrite to produce hydrogen. Near the exit of the WO reactor, we envision directing fresh steam over the reactant fins. The lower hydrogen partial pressure from the steam over the ferrite should enable the hydrolysis reaction to proceed further by maintaining nonequilibrium conditions.

A key feature of the CR5 is that it facilitates continuous removal and sweeping of the product gases. The moving reactants and the potential of fluidically establishing isolated reaction zones allow the solid and gas products to be separated. Furthermore, by a careful introduction of a sweep gas, it is possible to cause countercurrent flow between the sweep gas and the solid reactant. This ensures that the last environment seen by the solid reactant as it

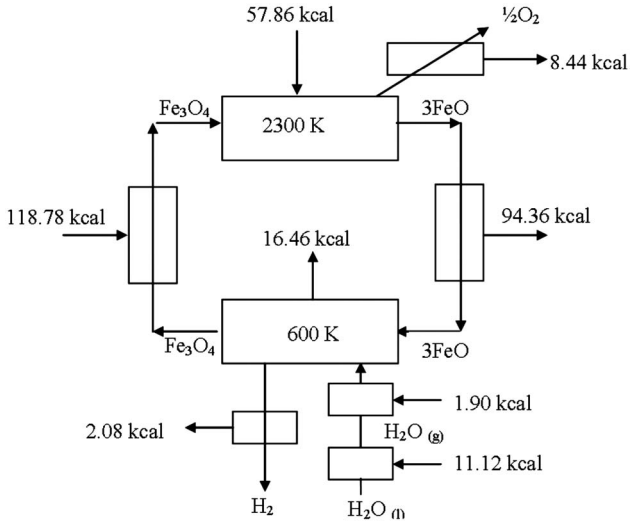

Fig. 2 Schematic showing heat flows of an ideal iron oxide cycle operating between 600 K and 2300 K

leaves the reactor is the most favorable thermodynamically for driving the reaction. The effectiveness of this approach, however, depends on fast reaction kinetics.

We envision using steam for sweeping. Nitrogen, argon, or other noncondensable gases require energy to separate and dramatically increase the pumping requirements for a subatmospheric operation. In the WO reactor, steam oxidizes the reduced ferrites and produces hydrogen. Increasing steam flow reduces the hydrogen partial pressure and increases the extent of reaction. With the oxidized ferrite in the TR reactor, steam is essentially inert and could be used as a sweep gas. However, we envision the use of little or no sweep gas in the TR reactor. Oxygen would be continually removed by pumping. A sweep gas results in an additional thermal parasitic load and could actually slow the TR reaction by inhibiting the mass transport of product oxygen from the surface. Thermal reduction kinetic studies of Fe_3O_4 indicate that the rate of reaction is limited by the gas phase mass transport of the O_2 from the surface [19]. Introducing small amounts of steam within the internal drives and/or within the recuperator is a way to counteract diffusion of product gases and mitigate crossover between the reactors.

Waste heat from the recuperator and hydrolysis reaction would be used to vaporize and preheat the water. Waste heat results from the exothermic WO reaction, recuperator inefficiencies, and sensible heat in the product hydrogen and oxygen. As in mechanical work producing heat engines, cooling of the low-temperature step and rejection of waste heat to the environment are required.

Sandia National Laboratories (SNL) is evaluating the practicality of the CR5 thermochemical heat engine. To assess the potential of the two-step ferrite cycle with the CR5, we have modeled the system performance. We are also numerically modeling various thermal and flow aspects of the CR5 and are trying to identify, engineer, and characterize redox materials/supports with the best possible thermodynamic and structural characteristics to establish whether suitable materials can be developed and fielded [20–22].

CR5 Cycle Thermodynamics

To understand the requirements for efficient two-step ferrite thermochemical cycles, it is instructive to consider simple thermodynamic models for the iron oxide system like that described by Nakamura [8]. Figure 2 is a simple model of the iron oxide system and illustrates some fundamental considerations. In it, iron oxide is cycled between 600 K—where it is reacted with steam in a WO reactor to produce hydrogen at 1 atm and magnetite (Fe_3O_4)—and 2300 K—where the magnetite is thermally reduced in a TR reactor to produce oxygen also at 1 atm, and wustite (FeO) as in Eqs. (1) and (2). For the purpose of illustration, we assume that 100% of the magnetite is converted to wustite and that the water/wustite has a reaction extent of 100%. (In reality, this is an unrealistically optimistic assumption at these temperatures and pressures.) Utilizing the thermodynamic data in HSC CHEMISTRY® for Windows (HSC) [23], we calculate that the amount of energy needed to heat the one mole of magnetite exiting the WO reactor from 600 K to 2300 K is 118.78 kcal. The amount of energy needed to drive the TR reaction to produce three moles of wustite and 1/2 mole of oxygen is 57.86 kcal; the amount of energy that needs to be rejected from the three moles of wustite to cool back to 600 K is 94.36 kcal; and the amount of exothermic heat that needs to be rejected from the hydrolysis reactor, where one mole of hydrogen is produced and one mole of magnetite is regenerated, is 16.46 kcal. In addition, 2.08 kcal of sensible heat in the product hydrogen and 8.44 kcal in the product oxygen need to be rejected. To heat and boil one mole of water from ambient (298.15 K) to produce water vapor at 373.15 K requires 11.12 kcal, and to heat it to 600 K requires another 1.90 kcal. The higher and lower heating values of the product hydrogen and oxygen are 68.31 kcal and 57.80 kcal, respectively. For comparison to heat engines, it is appropriate to base the output on the change in the Gibbs free energy, ΔG, of reaction, 56.68 kcal (liquid) or 54.63 kcal (gas) [5].

Without recuperation of the rejected heat, the amount of energy that must be supplied is $57.86+118.78+1.90+11.12=189.66$ kcal. If we define efficiency as the energy content in the product hydrogen and oxygen, the higher heating value (HHV) efficiency is at most $68.31/189.66=36.0\%$. If the round-trip reaction extent of magnetite to wustite and back is a more realistic 35%, then the amount of thermal energy needed to heat the magnetite from 600 K to 2300 K is $118.78/0.35=339.37$ kcal and the resulting HHV efficiency is only 16.7%. If the iron oxide is supported on a substrate such as zirconia, even more energy is required for sensible heating, and the efficiency is even lower.

With recuperation the amount of heat required can be substantially reduced. However, because of a pinch point that results from the different melting points of Fe_3O_4 (1870 K) and FeO (1650 K), the net heat required is not simply $57.86+118.78-94.36-8.44=73.84$ kcal. Instead, to ensure a positive temperature gradient throughout the recuperator, 89.88 kcal of solar energy must be added, resulting in a HHV efficiency of 76.0%. Without recuperating the high-temperature sensible heat in the product oxygen, a maximum HHV efficiency of 74.4% is possible (see the pinch-point diagram in Fig. 3). As Nakamura pointed out in Ref. [8], there is sufficient energy from the hydrolysis reaction to vaporize the water and preheat it to 600 K.

It is important to note that with efficient recuperation between the WO and TR reactors, the cycle can be efficient even with a less than complete reaction and with an inert support. In fact, assuming ideal recuperation, the ideal efficiencies above are theoretically possible with any level of conversion and mass of support. In reality, recuperation is never ideal, and achieving high conversion extent and minimizing the amount of inert support are important.

System Analysis

A simple system performance model was developed to understand the efficiency potential and requirements of the CR5 thermochemical heat engine. The system model includes a solar collection and a thermodynamic cycle model. For the thermodynamic cycle model, we developed conceptual CR5 engine designs to estimate the potential for recuperation and to understand other key design parameters. The designs assume 36 kW of net solar thermal energy delivered to the TR section of the reactor. The 36 kW is a nominal value for the 10 kW_e advanced dish development

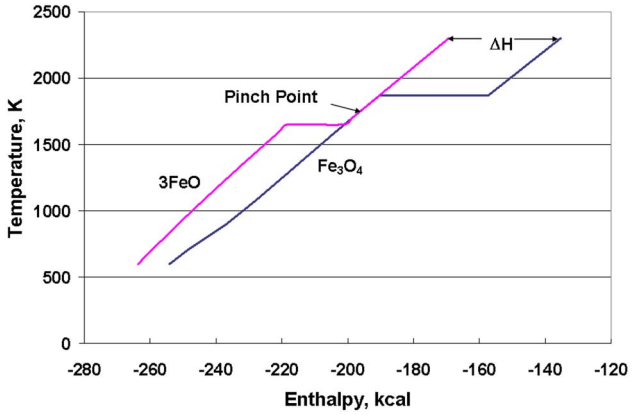

Fig. 3 Pinch-point diagram for an ideal iron oxide cycle operating between 600 K and 2300 K. The amount of sensible energy that must be added to the high-temperature step, ΔH, must be high enough to ensure a positive temperature gradient in all parts of the counter-current heat exchanger. In addition, the heat of reaction, 57.86 kcal, must also be added to the high-temperature step to convert a magnetite into a wustite.

systems (ADDSs) [3]. The ADDSs are dish/Stirling systems with high-performance parabolic dish concentrators suitable for the CR5.

Sample design parameters for a CR5 engine using iron oxide as a reactant material are listed in Table 1. In the design, the fin outside diameter is 0.61 m (24 in.). Recuperation heat rate, Q_r, was modeled, assuming radiation heat transfer according to Eq. (3) as in the analysis of radiation heat transfer between parallel plates.

$$Q_r = \sigma A F_{1-2}(T_1^4 - T_2^4)/((2/\varepsilon) - 1) \tag{3}$$

Based on the close proximity between fins, a fin-to-fin view factor, F_{1-2}, of 1.0 was assumed. A fin emissivity, ε, of 0.9 was also assumed. σ is the Stefan–Boltzmann constant. The recuperator radiation heat transfer area, A, was determined from the geometry of the 68 (34 pairs) of 25.4 mm (1 in.) tall fins. For these calculations the TR and WO reactor sections and the two recuperator sections each used one-quarter of the ring circumference. The ring spacing is 6.4 mm center to center (1/4 in.). This is the smallest spacing that we believe to be reasonable in a practical device. In the analysis, the recuperators are divided into 20 equal temperature-difference sections, and the average temperatures of each section are iteratively calculated by finding the temperature difference $(T_1 - T_2)$ between counter-rotating fins such that the recuperation heat rate in Eq. (3) for the 20 sections in the two recuperators equals the recuperator burden, Q_b, in

$$Q_b = \dot{m} c_p (T_{\text{approach}} - T_{\text{WO}}) \tag{4}$$

In Eq. (4), $\dot{m}$ is the mass flow rate of the reactant fins, c_p is the fin average heat capacity, T_{approach} is the temperature of the fins as they enter the TR reactor, and T_{WO} is the WO reactor temperature.

The use of an average fin heat capacity simplifies the analysis and means that $T_1 - T_2$ is constant across the recuperator and is equal to $T_{\text{TR}} - T_{\text{appraoch}}$. T_{TR} is the TR reactor temperature. Ring speeds of 0.5 to 1 rpm and reactant fin thicknesses on the order of 0.5 to 1 mm and containing 75 wt % zirconia (ZrO_2) are typical. With an estimated reactant fin density of 3500 kg/m^3, the void fraction of the fin stack is nearly 90%. Increasing the amount of the reactant fin material (reducing the fin void fraction) and proportionally reducing the ring speed result in the same performance and are potentially a way to increase the residence time in the WO and TR reactors to accommodate kinetics.

The thermodynamic cycle evaluations used HSC to evaluate ferrite spinels included in the HSC database to determine equilibrium compositions and state points across the reactors. The compositions in the reaction zones were calculated by iteratively solving for the equilibrium composition of the ferrite reactant alternately subjected to thermal reduction and hydrolysis at 1 atm and to the removal of the product oxygen and hydrogen, respectively. After several iterations, compositions did not change between iterations, and the extent of reaction, state-point properties, and thermal inputs could then be determined. With this approach and the HSC data, a TR temperature of 2300 K and a WO temperature of 600 K result in a reaction extent of 0.35 for Fe_3O_4. That is, for every mole of Fe_3O_4, 0.35 moles of hydrogen are produced. Comparable reaction extents could be obtained at 2100 K and 1900 K for Fe_2MgO_4 and Fe_2CoO_4, respectively, also at a WO reaction temperature of 600 K. It is important to note that this approach is conservative in that it does not account for the benefits of solid-gas reactions, e.g., the ability to drive the reaction by continuously removing the product gases. In calculating the state points, it is assumed that there are no reactions taking place in the recuperator. All of the thermal reduction occurs in the TR reactor. We also assume recuperation stops inside the reactor sections.

Although equilibrium is calculated at a pressure of 1 atm, it is assumed that the TR and WO reactors operate at 0.2 atm and that the oxygen is compressed to 1 atm and the hydrogen is compressed to 15 atm. We assume an isothermal compression efficiency of 40% at 300 K based on commercially available vacuum pump data.

Thermal efficiency is defined as

$$\eta_{\text{th}} = \frac{\dot{n}_{H_2} \times \text{HHV}_{H_2}}{Q_{\text{solar}} + \dot{W}_p/0.4} \tag{5}$$

where $\dot{n}_{H_2}$ is the molar hydrogen production rate, HHV_{H_2} is the higher heating value of hydrogen, Q_{solar} is the net solar power into the reactor (36 kW), and $\dot{W}_p$ is the compressor power. The compressor itself is assumed to be driven by a heat engine with a thermal-to-mechanical conversion efficiency of 40%. Power requirements for driving the counter-rotating rings are assumed to be negligible.

Table 2 lists the performance parameters for the iron oxide CR5 design outlined in Table 1. The net HHV thermal efficiency is 29.9%. Note that about 146 kW of power is required for sensible heating of the reactant, with most of it supplied by recuperation. (To heat the reactant, 125.06 kW is supplied by the recuperator, and an additional 20.96 kW of solar power is needed to heat it to temperature.) Only about 10% of the power needed for heating and reducing the oxidized ferrite actually drives the reaction (15.04 kW). With more effective recuperation, higher reaction ex-

Table 1 Baseline iron oxide CR5 heat engine design parameters

Design parameter	Value	Description
Q_{solar} (kW)	36	Net solar input into the TR reactor
T_{TR} (K)	2300	Temperature of the TR reactor
T_{WO} (K)	600	Temperature of the WO reactor
Pressure (atm)	0.2	Operating pressure
Fin outside diameter (m)	0.61	Outside diameter of the reactant fin
Fin inside diameter (m)	0.56	Inside diameter of the reactant fin
Fin height (mm)	25.4	Height of reactant fins
Ring spacing (mm)	6.4	Center-to-center ring spacing
Fin thickness (mm)	0.775	Thickness of the reactant fins
Ring speed (rpm)	0.75	rpm of the rings
Fin inert fraction	0.75	Reactant fin zirconia mass fraction
Fin average c_p (J/kg K)	800.8	Reactant fin average heat capacity
Fin density (kg/m^3)	3500	Reactant fin density
Reactor width (m)	0.43	Distance across rings
Number of rings	68	Number of rotating rings

Table 2 Baseline Fe_3O_4 CR5 heat engine performance parameters

Operational parameters	Value	Description
Recuperator ΔT (K)	244	Recuperator temperature difference
Recuperator effectiveness (%)	85.6	Percent of sensible energy in reactant fins recuperated
Recuperator power (kW)	125.06	Recuperator power for sensible heating of reactant fins
Average solar flux (W/cm^2)	17.44	Average incident solar flux on the TR section
Q receiver sensible (kW)	20.96	Amount of incident solar power for sensible heat to T_{TR}
Q receiver reaction (kW)	15.04	Amount of incident solar power for the TR reaction
Fin array porosity (%)	87.8	Apparent porosity of the volumetric reactant fin absorber
$\dot{m}$ (gm/s)	107.3	Mass flow rate of the reactant/zirconia material
Reaction extent (%)	35	Effective extent of reaction
$\dot{n}_{H_2}$ (moles H_2/s)	0.0412	Hydrogen production rate
l H_2/h	3320	Hydrogen production rate in standard l/h
HHV H_2 (kW)	11.77	Higher heating value rate of the produced hydrogen
Compressor power $\dot{W}_p$ (kW)	1.32	Pump power needed to compress the H_2 (15 atm) and O_2 (1 atm)
Gross efficiency (%)	32.7	H_2 HHV rate divided by the solar input
Net efficiency η_{th} (%)	29.9	H_2 HHV rate divided by the solar input plus power needed for pumps
Q hydrolysis (kW)	3.67	Exothermic power from the WO reactor
Q fin sensible (kW)	20.96	Rejected fin sensible power
Q reject (kW)	24.63	Total recuperator rejected power
Q H_2O (kW)	2.24	Power needed to vaporize and heat water to T_{WO}
Q O_2 sensible (kW)	1.49	Sensible power in oxygen stream
Q H_2 sensible (kW)	0.36	Sensible power in hydrogen stream

tent, and/or a reduced amount of inert carrier (ZrO_2), thermal efficiencies of up to about 50% are possible. The thermodynamic model also suggests that the product partial pressures need to be higher than about 0.1 atm. Otherwise, pump work becomes excessive. This means that the ferrite TR equilibrium oxygen and the WO hydrogen/steam partial pressures must be greater than 0.1 atm at operating conditions for this approach to be viable.

It is important to note that the potential for reducing the TR temperature or increasing the WO temperature by continuously removing the product gases by pumping or sweeping was not accounted for in this analysis. In this respect the results of our system efficiency studies are conservative. Because the extents of reaction depend on kinetics, we do not know how to properly account for this effect. Reducing the TR temperature and increasing the WO temperature to values similar to those currently being experimentally investigated (assuming no reduction in conversion) improves thermal efficiency. For example, changing the TR and WO temperatures to 1800 K and 1000 K, respectively, and assuming the same reaction extent, 0.35, for the example in the tables result in a HHV net thermal efficiency of over 44%. (This is intended to illustrate the importance of recuperation on efficiency. Although hydrogen production on a gram of material basis in this example is comparable to what has been demonstrated by Kodama et al. [15], whether or not this reaction extent can actually be obtained in a CR5 device at these temperatures needs to be demonstrated.) The reason that efficiency improves is that while the driving potential for recuperation decreases with reduced temperature (Eq. (3)), lower TR temperatures reduce the recuperator burden (Eq. (4)), especially if phase change can be avoided. Increasing the WO temperature increases the driving potential for recuperation and reduces the thermal burden on the recuperator. Figure 4 shows the calculated recuperator temperature profiles for the example in the tables. As can be seen in Fig. 4, recuperation at high temperatures requires less recuperator length than at low temperatures.

Ring speed is an important parameter. At low speeds recuperation efficiency improves. There is more time for transferring heat. However, if the ring speed is too low, the reactant flow rate is inadequate for the thermal input. We anticipate that for any given solar input, there exist optimum speeds for power and efficiency, not unlike conventional engines.

An analysis of collector efficiencies assuming an average concentration ratio of 4000 with 95% intercept, as demonstrated by the ADDS [3], indicates that operating temperatures of up to about 2100 K are practical from a solar collection efficiency perspective. Radiation losses from the solar receiver cavity are excessive at temperatures much higher than about 2100 K. From a system

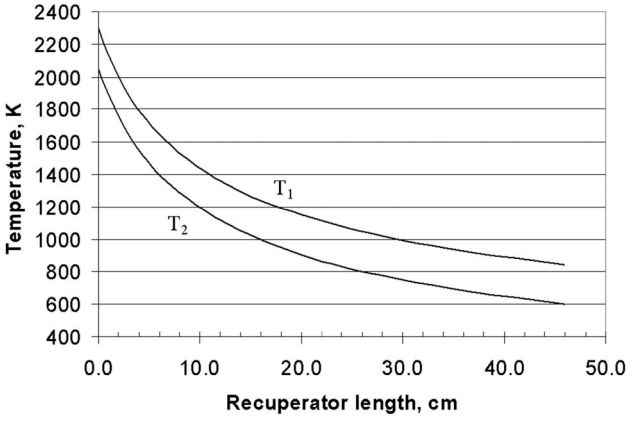

Fig. 4 Recuperator temperature profile for the case presented in Tables 1 and 2. Because of the constant heat capacity assumption, each incremental temperature has the same ΔH. Recuperation at high temperatures requires less of the recuperator than at low temperatures.

efficiency perspective, the mixed-metal ferrites and other approaches for reducing the TR temperature are, therefore, desirable. Furthermore, issues associated with volatilization and melting of the reactant material also encourage lower TR temperatures. Our HSC magnesium and cobalt ferrite results suggest that system efficiency can potentially be substantially better than a high-efficiency dish/Stirling system driving an electrolyzer.

CR5 Development Approach

The CR5 thermochemical heat engine concept and the underlying thermodynamics have many uncertainties. To better understand the practicality of the CR5 concept, we are evaluating key issues and are planning to build and test a prototype CR5 device.

Numerical simulations are being used to address key thermal and fluid dynamic aspects of the CR5. Because detailed radiation modeling in this device is extremely computer intensive and the kinetics are not known, we are not developing a comprehensive model incorporating radiation, chemical reactions, advection, multispecies flow, etc. Instead, our approach is to numerically model key aspects of the design, specifically recuperator performance and the potential for buoyancy-driven flow between reactors through the recuperators [20]. Benchmark comparisons of the simple recuperator submodel in the thermodynamic cycle model described above with a detailed recuperator model that accounts for solid-state heat conduction and uses temperature-dependent properties for candidate materials of construction and detailed enclosure radiation show good agreement. Because neither model accounts for conduction/convection heat transfer through the gas between fins or additional recuperation within the reactor sections, both of which can enhance recuperation, we have concluded that the counter-rotating-ring-recuperator concept is viable. To evaluate the potential for cross flow through the recuperator, separate flow models that use the results from the thermal model to define the temperature field were developed. We used the FLUENT computational fluid dynamics (CFD) code to simulate the flow field within the device [24]. The simulation was used primarily to assess the potential for buoyancy-driven flow through the recuperators. Because of the large temperature gradient and the orientation of the reactor during the operation, there is a chance that oxygen can cross from the TR reactor to the WO reactor. Results from the simulations indicate that ring rotation has no effect on crossover and that the potential for buoyancy-driven crossover is minor [20].

We are evaluating the thermodynamics of three promising iron ferrite systems based on Mg, Co, and Ni with another commercially available thermodynamic database called FactSage. The FactSage data represent the state of the art for spinel ferrites [25]. The calculations incorporate thermodynamic data for the nonideal solid- and liquid-phase solutions that form both the ferrites and their thermal decomposition products. The results indicate that complex solution phases form in addition to the ferrite, and the zirconia support is not completely inert. Some of the iron oxide and other metals in these systems form solutions with ZrO_2 and oxide solutions with each other. We are interested in the temperature and volume-dependent oxygen partial pressures to understand what is needed to meet the conditions identified in our system studies and the potential for pumping and sweeping to increase reaction extent. We are also interested in the effect of composition on the ferrite melting point, reaction extent, and hydrogen yields [22].

The CR5 design places unique demands on materials. The ferrite fins must maintain structural integrity and high reactivity over thousands of thermal cycles and exposure to temperatures in excess of 1700 K. In addition, the design of the fins must have a high surface area for gas-solid interactions and for absorption of incident solar radiation; it should also have high solar absorptivity. To address some of these requirements, we are characterizing the effect of a number of material parameters on performance in a test system for cyclic TR and WO with concurrent quantification of hydrogen and oxygen evolution. Although we have tested a number of ferrites, we have decided to focus mainly on a baseline cobalt ferrite to understand the design variables. Processing parameters such as synthesis procedure and particle size, as well as the impact of supporting the ferrite in a zirconia matrix, are of interest. Hydrogen and oxygen yields over successive cycles are the primary metrics. We are also applying characterization techniques such as x-ray diffraction, microscopy, and temperature programed reduction and oxidation to provide insights into the chemical and physical processes occurring in the ferrites during operation [21].

We are using robocasting, a Sandia-developed technique for free-form processing of ceramics to manufacture monolithic structures with complex three-dimensional geometries for chemical, physical, and mechanical evaluation [26]. We have demonstrated that ferrite/zirconia mixtures can be fabricated into small three-dimensional lattice structures; hydrogen and oxygen can be produced using these monolithic structures; and structural integrity can be maintained over successive cycles. Probably because of enhanced mass transport geometries, we have been able to produce more hydrogen and oxygen at faster rates with these monolithic structures than with equivalent amounts of powders. We have also fabricated reactant fin sections for the CR5 prototype. Design objectives for the fin sections include high geometric surface area, thermal shock resistance, and allowance for light penetration. The design of these monolithic structures is guided by our CFD studies. Figure 5 shows photographs of robocast: (*a*) a reactant ring assembly, (*b*) prototype reactant fin segments, (*c*) the test part as cast, and (*d*) the test part after 31 redox cycles. The cycling of the test part involved TR at approximately 1400°C and subsequent WO at about 1000°C [21].

A key result of our material studies is an appreciation of the importance of the zirconia support in enhancing the reduction reaction and avoiding issues associated with melting. Studies with iron oxide suspended in stabilized zirconia indicate that a small amount of the iron oxide would be expected to go into a solid solution with the zirconia support. It is possible that any remaining liquid iron oxide phase might "wet" or be suspended within the zirconia. In addition, the high oxygen mobility through zirconia may enhance kinetics. An important consequence is that high porosity may not be needed, and sintering of the porous zirconia may not be an issue. These observations appear to be in good agreement with those obtained by Ishihara et al. [16] and may be a key to the CR5 concept viability. They suggest a new type of redox material with high internal oxygen mobility for transport of oxygen to and from dispersed redox sites.

Given the numerous uncertainties, we believe that a proof-of-concept prototype CR5 thermochemical heat engine is needed to establish feasibility and to evaluate many of the unknowns. A proof-of-concept device with the overall objective of demonstrating the key features of the CR5 at a reasonable scale is being developed. It is designed to absorb approximately 9 kW of incident solar flux from the National Solar Thermal Test Facility (NSTTF) solar furnace in Albuquerque, NM. The design will be a first attempt to address high-temperature moving parts and other design issues. Ancillary hardware such as steam generation equipment and pumps and their integration into the system will not be addressed initially.

The prototype reactant rings have an outside diameter of 0.301 m (11.87 in.) and will utilize 2.34 cm (0.92 in.) tall reactant fins. The ring width is 1.27 cm (1/2 in.), and 14 rings will be used. Robocast ferrite fin segments will be attached to refractory ceramic fiber board supports and will be assembled into reactant rings. See Fig. 5(*a*). Rotation will be driven by two sets of internal gears. Two sets of sprocket gears will drive the rings. Sunlight will be introduced through a quartz-dome window, and steam will be ducted through ports in the insulation to provide countercurrent sweeping of the reactant fins. Design objectives include experimental flexibility and significant hydrogen production.

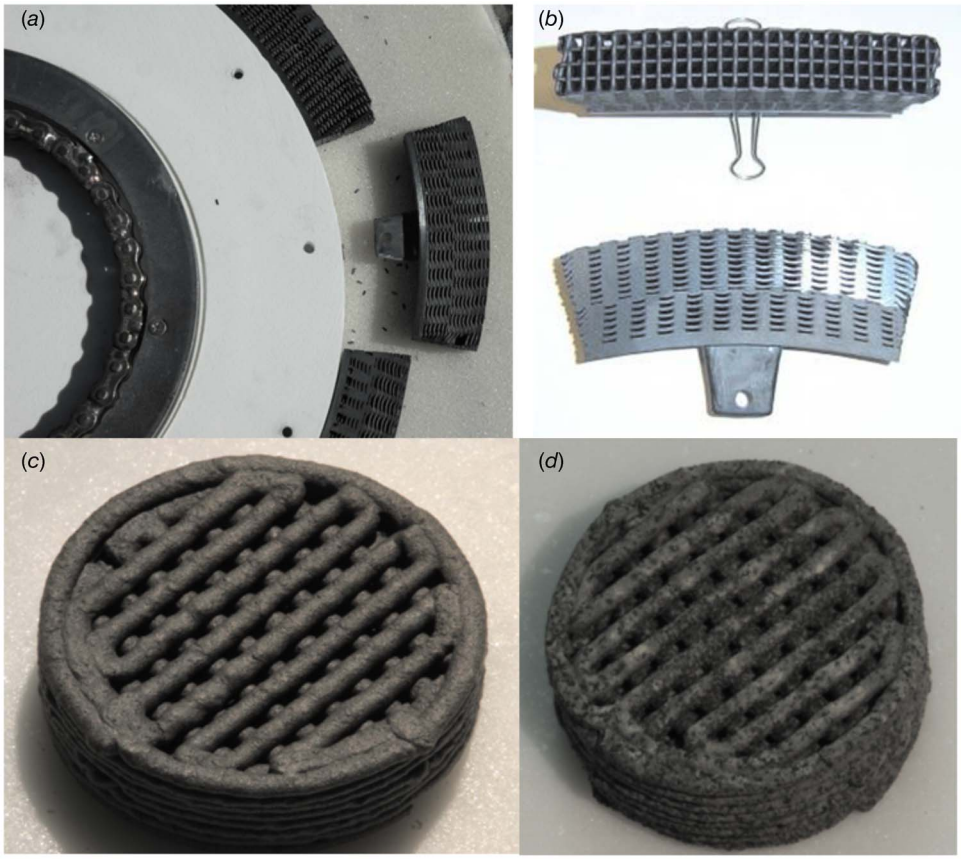

Fig. 5 Photograph of robocast: (*a*) reactant ring assembly, (*b*) prototype reactant fin segments, (*c*) as-cast cobalt ferrite/zirconia test sample, and (*d*) the cobalt ferrite/zirconia test sample after 31 thermal reduction and water oxidation cycles. The as-cast test sample is approximately 15 mm in diameter and 5.4 mm thick.

Conclusions

Solar hydrogen production from water by the use of two-step solar-driven thermochemical cycles is potentially an alternative to fossil fuels. Recognizing that thermochemical cycles are heat engines that convert thermal energy into chemical energy and are, therefore, analogous to mechanical work producing machines, we have conceived a new kind of heat engine. As in Stirling and Ericsson cycle mechanical work producing counterparts, countercurrent recuperation of sensible heat within the cycle is the key to high efficiency in the CR5. Investigations of the efficiency potential of the CR5 concept suggest that solid-to-solid countercurrent recuperation can be effective and that the cycle can potentially be efficient. Furthermore, recuperation mitigates the need for complete reaction extent and permits the use of support for the ferrite working material. These investigations also suggest that the underlying thermodynamic properties of the iron oxide redox materials are marginal at the temperatures dictated by materials and that a number of schemes will probably be required to compensate. These include adjusting the redox thermodynamics by substituting other metals for iron in the spinel, taking advantage of solid-gas reactions by continuous removal of the product gases, and effectively lowering the product gas partial pressure by countercurrent sweeping. Like other engines, the CR5 involves numerous design issues and tradeoffs. It places extraordinary demands on materials and involves high-temperature moving parts. In addition, the CR5 must be designed and operated to avoid a crossover through the recuperator. In the process of evaluating materials for the CR5 heat engine, we have developed a new kind of reactant material in which ferrite particles are dispersed in a monolithic zirconia structure. These materials appear to enhance and maintain reactivity and kinetics, as well as provide the structural support needed in the CR5 heat engine.

To establish the practicality of the CR5 concept, we are experimentally evaluating materials, exploring the thermodynamic design space, and evaluating fluid flow within the device. Given the potential, uncertainties, and results thus far, we have decided to design, build, and test a prototype device. If suitable materials can be developed and the design challenges can be met, the CR5 heat engine concept appears to provide an integrated approach for potentially efficient and low-cost solar hydrogen.

Acknowledgment

This work is supported by the U.S. Department of Energy under Contract No. DE-AC04-94-AL85000. The authors would like to acknowledge the contributions of John Stuecker, Lindsey Evans, Barry Boughton, and Darryl James.

Nomenclature

A = recuperator radiation heat transfer area (m^2)
c_p = average reactant fin heat capacity (J/kg K)
CR5 = counter-rotating-ring receiver/reactor/recuperator
F_{1-2} = view factor between recuperators
HHV_{H_2} = higher heating value of hydrogen (kcal/mole)
$\dot{m}$ = mass flow rate of reactant (gm/s)
$\dot{n}_{H_2}$ = hydrogen production rate (moles/s)
Q_b = recuperator burden (kW)

Q_r = recuperator heat transfer rate (kW)
Q_{solar} = net solar power (kW)
$T_{approach}$ = recuperator temperature at the entrance to the TR reactor (K)
T_{TR} = thermal reduction reactor temperature (K)
T_{WO} = water oxidation reactor temperature (K)
T_1 = heat emitting recuperator temperature (K)
T_2 = heat absorbing recuperator temperature (K)
$\dot{W}_p$ = compressor power (kW)
ε = fin emissivity
σ = Stefan–Boltzmann constant (5.668×10^{-8} W/m^2 K^4)
η_{th} = thermal efficiency (%)

References

[1] Dunn, S., 2001, *Hydrogen Futures: Toward a Sustainable Energy System*, Worldwatch Paper 157, Worldwatch Institute, Washington, D.C.

[2] O'Gallagher, J. J., and Lewandowski, A., 2005, "Achieving Ultra-High Solar Concentration for the Production of Hydrogen in a Central Receiver Plant Using a Nonimaging CPC Type Secondary," *Proceedings of the ASES 2005 Solar World Congress*, Orlando, FL, Aug. 6–12.

[3] Diver, R. B., Andraka, C. E., Rawlinson, K. S., Goldberg, V., and Thomas, G., 2001, "The Advanced Dish Development System Project," *ASME Proceedings of Solar Forum 2001*, Washington, D.C., Apr. 21–25.

[4] National Academies of Science Report to DOE, 2002, "Critique of the Sargent and Lundy Assessment of Cost and Performance Forecasts for Concentrating Solar Power Technology," Washington, D.C.

[5] Fletcher, E. A., and Moen, R. L., 1977, "Hydrogen and Oxygen From Water," Science, **197**, pp. 1050–1056.

[6] Brown, L., Besenbruch, G. E., Chen, Y., Diver, R., Earl, B., Hsieh, S., Kwan, K., McQuillan, B. W., Perkins, C., Pohl, P., and Weime, A., 2005, "A Database of Solar Thermochemical Hydrogen Cycles," *Proceedings of the National Hydrogen Association*, Washington, D.C., Mar. 29–31.

[7] Brown, L. C., Funk, J. F., and Showalter, S. K., 2000, "High Efficiency Generation of Hydrogen Fuels Using Nuclear Power," Report No. GA-A23451.

[8] Nakamura, T., 1977, "Hydrogen Production From Water Utilizing Solar Heat at High Temperatures," Sol. Energy, **19**, pp. 467–475.

[9] Lundberg, M., 1993, "Model Calculations on Some Feasible Two-Step Water Splitting Processes," Int. J. Hydrogen Energy, **18**(5), pp. 369–376.

[10] Tamura, Y., Steinfeld, A., Kuhn, P., and Ehrensberger, K., 1995, "Production of Solar Hydrogen by a Novel, 2-Step, Water-Splitting Thermochemical Cycle," Energy, **20**(4), pp. 325–330.

[11] Steinfeld, A., Kuhn, P., Reller, A., Palumbo, R., Murry, J., and Tamaura, Y., 1998, "Solar-Processed Metals as Clean Energy Carriers and Water-Splitters," Int. J. Hydrogen Energy, **23**(9), pp. 767–774.

[12] Ehrensberger, K., Frei, A., Kuhn, P., Oswald, H. R., and Hug, P., 1995, "Comparative Experimental Investigations of the Water-Splitting Reaction With Iron Oxide $Fe_{1-y}O$ and Iron Manganese Oxides $(Fe_{1-x}Mn_x)_{1-y}O$," Solid State Ionics, **78**, pp. 151–160.

[13] Aoki, H., Kaneko, H., Hasegawa, N., Ishihara, H., Takahashi, Y., Suzuki, A., and Tamaura, Y., 2004, "Two-Step Water Splitting With Ni-Ferrite System for Solar H2 Production Using Concentrated Solar Radiation," *Proceedings of ISES 2004 in Solar 2004, ASME: International Solar Energy Conference*, Portland, OR, July 11–14.

[14] Kodama, T., Kondoh, Y., Kiyama, A., and Shimizu, K., 2003, "Hydrogen Production by Solar Thermochemical Water-Splitting/Methane-Reforming Process," *Proceedings of the ASME ISES Conference*, Hawaii, Mar. 15–18.

[15] Kodama, T., Kondoh, Y., Yamamoto, R., Andou, H., and Satou, N., 2005, "Thermochemical Hydrogen Production by Redox System of ZrO2-Supported Co(II)-Ferrite," Sol. Energy, **78**, pp. 623–631.

[16] Ishihara, H., Kaneko, H., Yokoyama, T., Fuse, A., and Tamaura, Y., 2005, "Hydrogen Production Through Two-Step Water Splitting Using YSZ (Ni, Fe) System for Solar Hydrogen Production," *Proceedings of ISEC 2005 International Solar Energy Conference*, Orlando, FL, Aug. 6–12.

[17] Kaneko, H., Miura, T., Fuse, A., Ishihara, H., Taku, S., Fukuzumi, H., Naganuma, Y., and Tamaura, Y., 2007, "Rotary-Type Solar Reactor for Solar Hydrogen Production With Two-step Water Splitting Process," Energy Fuels, **21**, pp. 2287–2293.

[18] Roeb, M., Sattler, C., Kluser, R., Monnerie, L., Konstandopoulos, A. G., Agrafiotis, C., Zaspalis, V. T., Nalbandian, L., Steele, A., and Stobbe, P., 2005, "Solar Hydrogen Production by a Two-Step Cycle Based on Mixed Iron Oxides," *ASME Proceedings ISEC 2005 International Solar Energy Conference*, Orlando, FL, Aug. 6–12.

[19] Steinfeld, A., Sanders, S., and Palumbo, R., 1999, "Design Aspects of Solar Thermochemical Engineering—A Case Study: Two-Step Water-Splitting Cycle Using the Fe_3O_4/FeO Redox System," Sol. Energy, **65**(1), pp. 43–53.

[20] James, D. L., Siegel, N. P., and Diver, R. B., Boughton, B. D., and Hogan, R. E., 2006, "Numerical Modeling of Solar Thermochemical Water Splitting Reactor," *Proceedings of the ASME Solar Energy Conference 2006*, Denver, CO, July 8–13.

[21] Miller, J. E., Evans, L. R., Stuecker, J. N., Allendorf, M. D., Siegel, N. P., and Diver, R. B., 2006, "Materials Development for the CR5 Solar Thermochemical Heat Engine," *Proceedings of the ASME Solar Energy Conference 2006*, Denver, CO, July 8–13.

[22] Allendorf, M. D., Miller, J. E., Siegel, N. P., and Diver, R. B., 2006, "Thermodynamic Analysis of Mixed-Metal Ferrites for Hydrogen Production by Two-Step Water Splitting," *Proceedings of the ASME Solar Energy Conference 2006*, Denver, CO, July 8–13.

[23] Roine, A., 2002, HSC 5, Version 5.1, computer program, Outokumpu HSC Chemistry for Windows; Report No. 02103-ORC-T.

[24] 2005, FLUENT, Version 6.2, Fluent Inc.

[25] Bale, C. W., Chartrand, P., Degterov, S. A., Eriksson, G., Hack, K., Mahfoud, R. B., Melançon, J., Pelton, A. D., and Petersen, S., 2002, "FactSage Thermochemical Software and Databases," CALPHAD: Comput. Coupling Phase Diagrams Thermochem., **26**, pp. 189–228.

[26] Cesarano, J., III, Segalman, R., and Calvert, P., 1998, "Robocasting Provides Moldless Fabrication From Slurry Deposition," Ceram. Ind., **148**, pp. 94–102.